A fresh look at *Cladarosymblema,* a tetrapod-like fish from the Carboniferous of Australia, illuminated via X-ray tomography (#66190)

First submission

Guidance from your Editor

Please submit by **13 Oct 2021** for the benefit of the authors (and your $200 publishing discount) .

Structure and Criteria
Please read the 'Structure and Criteria' page for general guidance.

Author notes
Have you read the author notes on the guidance page?

Raw data check
Review the raw data.

Image check
Check that figures and images have not been inappropriately manipulated.

Privacy reminder: If uploading an annotated PDF, remove identifiable information to remain anonymous.

Files

Download and review all files from the materials page.

8 Figure file(s)
1 Video file(s)
1 Raw data file(s)

Structure and Criteria

Structure your review

The review form is divided into 5 sections. Please consider these when composing your review:

1. **BASIC REPORTING**
2. **EXPERIMENTAL DESIGN**
3. **VALIDITY OF THE FINDINGS**
4. General comments
5. Confidential notes to the editor

📄 You can also annotate this PDF and upload it as part of your review

When ready [submit online](#).

Editorial Criteria

Use these criteria points to structure your review. The full detailed editorial criteria is on your [guidance page](#).

BASIC REPORTING

- Clear, unambiguous, professional English language used throughout.
- Intro & background to show context. Literature well referenced & relevant.
- Structure conforms to [PeerJ standards](#), discipline norm, or improved for clarity.
- Figures are relevant, high quality, well labelled & described.
- Raw data supplied (see [PeerJ policy](#)).

EXPERIMENTAL DESIGN

- Original primary research within [Scope of the journal](#).
- Research question well defined, relevant & meaningful. It is stated how the research fills an identified knowledge gap.
- Rigorous investigation performed to a high technical & ethical standard.
- Methods described with sufficient detail & information to replicate.

VALIDITY OF THE FINDINGS

- Impact and novelty not assessed. *Meaningful* replication encouraged where rationale & benefit to literature is clearly stated.
- All underlying data have been provided; they are robust, statistically sound, & controlled.

- Conclusions are well stated, linked to original research question & limited to supporting results.

Standout reviewing tips

The best reviewers use these techniques

Tip	Example
Support criticisms with evidence from the text or from other sources	*Smith et al (J of Methodology, 2005, V3, pp 123) have shown that the analysis you use in Lines 241-250 is not the most appropriate for this situation. Please explain why you used this method.*
Give specific suggestions on how to improve the manuscript	*Your introduction needs more detail. I suggest that you improve the description at lines 57- 86 to provide more justification for your study (specifically, you should expand upon the knowledge gap being filled).*
Comment on language and grammar issues	*The English language should be improved to ensure that an international audience can clearly understand your text. Some examples where the language could be improved include lines 23, 77, 121, 128 – the current phrasing makes comprehension difficult. I suggest you have a colleague who is proficient in English and familiar with the subject matter review your manuscript, or contact a professional editing service.*
Organize by importance of the issues, and number your points	*1. Your most important issue* *2. The next most important item* *3. ...* *4. The least important points*
Please provide constructive criticism, and avoid personal opinions	*I thank you for providing the raw data, however your supplemental files need more descriptive metadata identifiers to be useful to future readers. Although your results are compelling, the data analysis should be improved in the following ways: AA, BB, CC*
Comment on strengths (as well as weaknesses) of the manuscript	*I commend the authors for their extensive data set, compiled over many years of detailed fieldwork. In addition, the manuscript is clearly written in professional, unambiguous language. If there is a weakness, it is in the statistical analysis (as I have noted above) which should be improved upon before Acceptance.*

A fresh look at *Cladarosymblema,* a tetrapod-like fish from the Carboniferous of Australia, illuminated via X-ray tomography

Alice M Clement [Corresp., 1] , **Richard Cloutier** [2] , **Jing Lu** [3, 4] , **Egon Perilli** [1] , **Anton Maksimenko** [5] , **John A Long** [1]

[1] College of Science and Engineering, Flinders University of South Australia, Adelaide, South Australia, Australia

[2] Département de Biologie, Chimie et Géographie, University of Québec at Rimouski, Rimouski, Quebec, Canada

[3] Key Laboratory of Vertebrate Evolution and Human Origins of Chinese Academy of Sciences, Institute of Vertebrate Paleontology and Paleoanthropology, Beijing, China

[4] CAS Center for Excellence in Life and Paleoenvironment, Beijing, China

[5] Australian Synchrotron, Australian Nuclear Science and Technology Organisation, Melbourne, Victoria, Australia

Corresponding Author: Alice M Clement
Email address: alice.clement@flinders.edu.au

Background. The megalichthyids are one of several clades of extinct tetrapod-like fish that lived throughout the Devonian – Permian periods. They are advanced 'osteolepid-grade' fishes that lived in freshwater swamp and lake environments, with some taxa growing to very large sizes. They bear cosmine-covered bones and a large premaxillary tusk that lies lingually to a row of small teeth. Diagnosis of the family remains controversial with various authors revising it several times in recent works. There are fewer than 10 genera known globally, and only one member identified from Gondwana. *Cladarosymblema narrienense* Fox et al. 1995 was described from the Lower Carboniferous Raymond Formation in Queensland, Australia, on the basis of several well-preserved specimens. Despite this detailed work, several aspects of its anatomy remain undescribed.

Methods. Two especially well-preserved 3D fossils of *Cladarosymblema*, including the holotype specimen, are scanned using synchrotron or micro-computed tomography (μCT), and 3D modelled using specialist segmentation and visualisation software. New anatomical detail, in particular internal anatomy, is revealed for the first time in this taxon. A novel phylogenetic matrix, adapted from other recent work on tetrapodomorphs, is used to clarify the interrelationships of the megalichthyids and confirm the phylogenetic position *Cladarosymblema*.

Results. Never before seen morphological details of the palate, hyoid arch, basibranchial skeleton, pectoral girdle and axial skeleton are herein revealed and described. Several additional features are confirmed or updated from the original description. Moreover, we present and describe the first full, virtual cranial endocast of any tetrapodomorph fish, giving insight into the early neural adaptations in this group. Phylogenetic analysis confirms the monophyly of the Megalichthyidae with seven genera included (*Askerichthys, Cladarosymblema, Ectosteorhachis, Mahalalepis, Megalichthys, Palatinichthys,* and *Sengoerichthys*). The position of the megalichthyids as sister group to canowindrids, crownward of 'osteolepidids' (e.g. *Osteolepis* and *Gogonasus*), but below tristichopterids such as *Eusthenopteron* is confirmed, but our findings suggest further work is required to resolve megalichthyid interrelationships.

1 **A fresh look at *Cladarosymblema,* a tetrapod-like fish from**

2 **the Carboniferous of Australia, illuminated via X-ray**

3 **tomography**

4

5 Alice M. Clement[1*], Richard Cloutier[2], Jing Lu[3,4], Egon Perilli[1], Anton Maksimenko[5] & John A. Long[1]

6

7 *[1] College of Science & Engineering, Flinders University, Adelaide, AUSTRALIA*

8 *[2] Université du Québec à Rimouski, Rimouski, Quebec, CANADA*

9 *[3] Key Laboratory of Vertebrate Evolution and Human Origins of Chinese Academy of Sciences,*

10 *Institute of Vertebrate Paleontology and Paleoanthropology, Chinese Academy of Sciences, Beijing,*

11 *CHINA*

12 *[4] CAS Center for Excellence in Life and Paleoenvironment, Beijing, CHINA*

13 *[5] Australian Synchrotron, Australian Nuclear Science and Technology Organisation, Melbourne,*

14 *AUSTRALIA*

15

16 Corresponding Author: Alice M. Clement[1*]

17 Flinders University, Sturt Road, Bedford Park, Adelaide, 5042, Australia.

18 Email: alice.clement@flinders.edu.au

19

20

21 ABSTRACT

22 **Background.** The megalichthyids are one of several clades of extinct tetrapod-like fish that lived

23 throughout the Devonian – Permian periods. They are advanced 'osteolepid-grade' fishes that lived

24 in freshwater swamp and lake environments, with some taxa growing to very large sizes. They bear

25 cosmine-covered bones and a large premaxillary tusk that lies lingually to a row of small teeth.

26 Diagnosis of the family remains controversial with various authors revising it several times in recent

27 works. There are fewer than 10 genera known globally, and only one member identified from

28 Gondwana. *Cladarosymblema narrienense* Fox et al. 1995 was described from the Lower

29 Carboniferous Raymond Formation in Queensland, Australia, on the basis of several well-preserved

30 specimens. Despite this detailed work, several aspects of its anatomy remain undescribed.

31 **Methods.** Two especially well-preserved 3D fossils of *Cladarosymblema*, including the holotype

32 specimen, are scanned using synchrotron or micro-computed tomography (μCT), and 3D modelled

33 using specialist segmentation and visualisation software. New anatomical detail, in particular

34 internal anatomy, is revealed for the first time in this taxon. A novel phylogenetic matrix, adapted

35 from other recent work on tetrapodomorphs, is used to clarify the interrelationships of the

36 megalichthyids and confirm the phylogenetic position *Cladarosymblema*.

37 **Results.** Never before seen morphological details of the palate, hyoid arch, basibranchial skeleton,
38 pectoral girdle and axial skeleton are herein revealed and described. Several additional features are
39 confirmed or updated from the original description. Moreover, we present and describe the first full,
40 virtual cranial endocast of any tetrapodomorph fish, giving insight into the early neural adaptations
41 in this group. Phylogenetic analysis confirms the monophyly of the Megalichthyidae with seven
42 genera included (*Askerichthys, Cladarosymblema, Ectosteorhachis, Mahalalepis, Megalichthys,*
43 *Palatinichthys,* and *Sengoerichthys*). The position of the megalichthyids as sister group to
44 canowindrids, crownward of 'osteolepidids' (e.g. *Osteolepis* and *Gogonasus*), but below
45 tristichopterids such as *Eusthenopteron* is confirmed, but our findings suggest further work is
46 required to resolve megalichthyid interrelationships.

KEY WORDS

50 Sarcopterygii; tetrapodomorph; Megalichthyidae; Carboniferous; tomography; endocast.

INTRODUCTION

54 Megalichthyids are an extinct clade of sarcopterygian (lobe-finned) tetrapod-like fishes known from
55 the Palaeozoic. They appeared in the Mid-Late Devonian, and were one of the few sarcopterygian
56 groups that survived the end-Devonian extinctions, persisting up until the Lower Permian (Witzmann
57 & Schoch 2012). They fall within a 'osteolepid-grade' in most phylogenetic analyses of stem-
58 tetrapod interrelationships (Ahlberg & Johanson 1998; Cloutier et al. 2020; Johanson 2004; Johanson
59 & Ahlberg 2001; Lu et al. 2012; Zhu & Ahlberg 2004; Zhu et al. 2017). They are typically recovered
60 most closely related to the East Gondwanan endemic group the Canowindridae (*Beelarongia,*
61 *Koharalepis, Canowindra*), usually crownward of rhizodonts and basal of the tristichopterids (such as
62 *Eusthenopteron*) and the elpistostegalian fishes.

63 Hay (1902) was the first to coin the term 'Megalichthyidae', after which Long (1985) suggested
64 synapomorphies to define the clade, but the first full familial description was not provided until
65 Young et al. (1992). This was later revised by Fox et al. (1995), Borgen and Nakrem (2016), and again
66 most recently by Downs and Daeschler (2020).

67 In describing a new species of *Megalichthys* (*M. mullisoni*) from the Famennian of USA, Downs and
68 Daeschler (2020) reduced the characters defining the family to three specialised features in
69 combination with one plesiomorphic character: cosmine cover on dermal bones; premaxillary tusk
70 that interrupts or lies lingual to the premaxillary marginal tooth row; contact between the
71 subopercular and second submandibular; and a distinct supratemporal bone.

72 The family Megalichthyidae includes a handful of taxa from Europe, Russia, Middle East, and North
73 America, but there is only one taxon described from Australia. *Cladarosymblema narrienense* (Fox et
74 al. 1995) is known from the Lower Carboniferous (Viséan) Raymond Formation in Queensland,
75 Australia, and is the only megalichthyid described from the Southern Hemisphere (Long et al. 2018).

76   Aside from *Cladarosymblema*, there are several other genera commonly recognised within the
77   Megalichthyidae: *Megalichthys* (Agassiz 1835) contains several species found in Carboniferous
78   deposits across North America, Morocco, the UK, and Europe; *Ectosteorhachis* (Cope 1882) is known
79   from the Lower Permian of the US; *Sengoerichthys* -considered by some as the earliest
80   megalichthyid- from the Frasnian of Turkey (Janvier et al. 2007); *Palatinichthys* described from the
81   Lower Permian of Germany (Witzmann & Schoch 2012); and the most recently described
82   megalichthyid genus, *Askerichthys,* comes from the Late Carboniferous of Norway (Borgen & Nakrem
83   2016). However, Downs and Daeschler (2020) considered that the "unusual combinations of
84   characters" in *Sengoerichthys* and *Palatinichthys* precluded them from being megalichthyids.

85   Several other taxa have been considered at times to share affinities with the megalichthyids, but are
86   usually excluded from most analyses due to lacking diagnostic family features or by being too poorly
87   known. Namely, Fox et al. (1995), Janvier et al. (2007) and Witzmann & Schoch (2012) excluded the
88   lesser-known taxa *Lohsania* (Thomson & Vaughn 1968), *Megistolepis* and *Megapomus* (Vorobyeva
89   1977), *Cryptolepis* (Lebedev 1995; Vorobyeva 1975), and *Mahalalepis* (Young et al. 1992) from their
90   studies. The Middle-Late Devonian *Mahalalepis*, from Mount Crean in Antarctica, was named from a
91   single fronto-ethmoidal shield but was considered by Young et al. (1992) to be a megalichthyid. If
92   accepted as a megalichthyid, it would represent the oldest member of the clade. Additional material
93   is currently under description and will likely soon more conclusively clarify its taxonomic affinities
94   (Jing Lu, pers. comm.)

95   In contrast to some of the taxa named above, *Cladarosymblema* is well known, described on the
96   basis of several 3D-preserved specimens exposed by acid-etching and mechanical preparation. Fox
97   et al. (1995) described in detail many aspects of its anatomy - including the dermal skull bones,
98   braincase, mandible, pectoral girdle and fin, limited elements of the axial skeleton and hyoid arch, as
99   well as the teeth and scales. However, the accessibility of modern scanning techniques today now
100   permits a detailed re-examination of *Cladarosymblema* to illuminate features of its morphology that
101   have until now remained elusive. Herein we use high-resolution micro-CT (μCT) and synchrotron
102   tomography to reveal unseen features not previously described, including elements of the hyoid
103   arch, palatal bones, axial skeleton and a cranial endocast. In doing so we uncover several aspects of
104   its morphology that prove useful for supporting a more robust clade of the Megalichthyidae, and
105   provide broader resolution in phylogenetic analyses of the problematic 'osteolepid-grade' of
106   Palaeozoic tetrapod-like fishes.

107

108

109   **MATERIAL & METHODS**

110   **Material**

111   Two exceptionally preserved specimens of the megalichthyid, *Cladarosymblema narrienense*, from
112   the Lower Carboniferous Raymond Formation of the Officer Basin, Queensland, Australia, were
113   scanned using a cabinet micro-CT or synchrotron tomography to reveal new internal anatomical
114   detail.

115   The holotype is a Queensland Museum specimen (QMF 21082) preserved in a single block of silty
116   limestone and contains the skull, anterior trunk region and both pectoral fins, described in detail by

117   Fox et al. (1995). Several bones from the left side of the specimen were removed during preparation
118   so not all paired elements are present on both sides of the specimen, and consequently the right
119   side is the more complete. There are reinforcing metal wires surrounding the perimeter of both
120   pectoral fins.

121   The second specimen (~50 mm length, ~40 mm width) is an isolated ethmosphenoid from the
122   Queensland Museum collection (QMF 21083). This specimen has been acid-prepared, and retains
123   small sections of in-filled limestone within the cranial cavity. There is some slight compression
124   internally but the nasal capsules and hypophyseal region of the endocranium are well preserved.

125

126   **Scanning & Segmentation**

127   The holotype (QMF 21082), although relatively large (dimensions approximately 230 mm length, 200
128   mm width, 35 mm height), was able to be scanned in 2020 at the Flinders University micro-CT
129   Laboratory using a large-volume micro-CT system (Nikon XTH225 ST, Nikon Metrology Tring,
130   Hertfordshire, UK). The specimen was placed in a polystyrene-foam box (transparent to X-rays), with
131   the long specimen axis vertically aligned with the rotation axis of the micro-CT rotation stage. The
132   specimen was scanned using the following parameters: 160 kV; 282 µA (45W), 0.25 mm tin filter,
133   2.83 s exposure, rotation step 0.1° over 360°; with a resulting voxel size of 58µm (4056 x 4056 pixel
134   detector), containing the entire specimen in the field of view (SI-Figure 1e). The tomographic cross-
135   sections were reconstructed using a filtered back-projection algorithm (Nikon CT Pro 3D software)
136   and saved as 8-bit bitmap format images. A stack of up to 4000 consecutive cross sections was
137   reconstructed, resulting in a height of up to 232 mm. Each cross-section was 3000 x 1100 pixels
138   (corresponding to 174 x 63.8 mm) in size, producing a dataset occupying 12.4 GB in hard drive space.
139   Images were later subsampled by a factor two to a voxel size of 116µm (Perilli et al. 2012).

140   An isolated ethmosphenoid (QMF 21083) was scanned in 2016 at the Australian Nuclear Science and
141   Technology Organisation (ANSTO) Australian Synchrotron in Melbourne (experiment number
142   AM10403) using the following parameters: 50 kV, 181° deg., 1810 projections; angle step 0.1°;
143   exposure time 0.22 sec; object to detector 35 mm; with a resultant voxel size of 12.2µm. This initially
144   produced a dataset occupying 25.3 GB hard drive space, but was rescaled to an eventual 6.3 GB
145   dataset in ImageJ.

146   Reconstructed scan data and associated derived files are deposited on MorphoSource at:
147   https://www.morphosource.org/dashboard/collections/000383372/edit?locale=en, or see SI-Figure
148   1 for example reconstructed tomographic slice data. Data were segmented manually using
149   thresholding and rendered in MIMICS V. 18 & v.19 (Materialise, Leuven, Belgium;
150   http://biomedical.materialise.com/mimics), animations were compiled in Adobe Premier Pro.

151

152   **Phylogenetic Analysis**

153   The phylogenetic position of the megalichthyids among tetrapodomorphs, as well as the
154   interrelationships among megalichthyids are investigated using the tetrapodomorph character
155   matrix of Cloutier et al. (2020). Cloutier et al.'s (2020) phylogenetic data matrix (comprising 202

156   characters coded for 43 taxa) was based on 169 characters from Zhu et al. (2017), 13 characters
157   from Daeschler et al. (2006), 11 characters from Swartz (2012) and 5 characters from Cloutier et al.
158   (2020). The new matrix includes 48 taxa. Four new characters are added to Cloutier et al.'s (2020)
159   matrix: characters 203 [Long medioventral process of premaxilla: (0) absent; (1) present]; 204
160   [Relative size of anterior tectal and lateral rostral: (0) lateral rostral much larger than anterior tectal,
161   (1) lateral rostral and anterior tectal equidimensional, (2) lateral rostral smaller than anterior tectal];
162   205 [Size of bones forming the external nares: (0) anterior tectal and lateral rostral similar in size to
163   the posterior tectal, (1) anterior tectal and lateral rostral much smaller than the posterior tectal];
164   and lastly 206 [Anterolateral process of supratemporal: (0) absent, (1) present].

165   Simões and Pierce (2021) changed two codings from Cloutier et al.'s (2020) matrix: character 62
166   (anteromedial process of vomer) for *Acanthostega* and character 106 (opercular process of
167   hyomandibula) for *Panderichthys*. We solely agree with the modification suggested for the coding of
168   *Acanthostega* for character 62.

169   To the original matrix we included five megalichthyids or taxa assigned to be likely megalichthyids:
170   *Sengoerichthys ottoman* (Janvier et al. 2007), *Palatinichthys laticeps* (Witzmann & Schoch 2012),
171   *Askerichthys heintzi* (Borgen & Nakrem 2016), *Mahalalepis resima* (Young et al. 1992), and
172   *Megalichthys mullisoni* (Downs & Daeschler 2020). In addition, we recoded *Cladarosymblema* based
173   on our new morphological description presented herein, with additional codings for *Mahalalepis*
174   based on work currently in preparation (Jing Lu, IVPP, pers. comm.) Rather than entering
175   *Megalichthys* as a composite taxon, we coded for *M. hibberti* and *M. laticeps* in addition to *M.*
176   *mullisoni* as separate species.

177   Thus, we performed parsimony analyses on our matrix (http://morphobank.org/permalink/?P3818),
178   which was coded for 49 taxa (including 5 outgroups) and 206 characters using a heuristic search.
179   Additional comments on codings are contained within the matrix on Morphobank. The tree was
180   rooted on a constrained monophyletic outgroup composed of *Youngolepis, Diabolepis*, *Powichthys,*
181   *Porolepis*, and *Glyptolepis*. A total of 18 multi-state characters were run ordered; in addition to the
182   morphocline defined in Cloutier et al. (2020, supplementary information) character 204 was
183   considered as a morphocline. Strict, Adams and 50% majority consensus trees were computed. All
184   analyses were performed in PAUP*v4.0a.

185

186

187   **DESCRIPTION**

188   **The Dermal Skull**

189   On the skull roof, the course of the lateral line canal can be confirmed as lyre-shaped (Fig. 1). It lies
190   close to associated pore group clusters, which are considered likely electroreceptors following the
191   work by King et al. (2018). A network of tubuli in the snout region provide further evidence that
192   *Cladarosymblema* likely had some electroreceptive ability. A single bone posterior and disarticulated
193   from the skull roof is confirmed as the median extrascapular due to the presence of the mesial otic
194   sensory-line canal running through it, with no junction for the main otic sensory canal as would be
195   expected in the lateral bones. The cheek bones were described by Fox et al. (1995) and follow a

196   standard basal tetrapodomorph arrangement. Those on the holotype are imperfectly preserved so
197   will not be considered further.

198   Concerning the gulars and submandibular bones (Fig. 2), Fox et al. (1995) described the lateral
199   (principal) gular of the holotype to have width of 40% of its total length, but we find its width to be
200   closer to 35%. We herein confirm that there was little to no overlap area in its posteromedial corner
201   for the other gular bone. The median gular is about 30% of the length of the lateral gulars, thus
202   slightly smaller than the condition in *Askerichthys* (c.40%). There are in fact seven submandibulars in
203   the holotype, as in *Megalichthys* and *Ectosteorhachis*, although the penultimate one is broken in
204   half. This contrasts with *Palatinchthys* which has three submandibulars (Witzmann & Schoch 2012),
205   and *Askerichthys* which has six (Borgen & Nakrem 2016). There is an area for overlap with the
206   subopercular on the first submandibular only. We find no evidence of a groove on the underside of
207   the operculum as seen on QMF21105 (Fox et al. 1995). A reconstruction of the dermal skeleton of
208   *Cladarosymblema* in lateral view is shown in Figure 2e, synthesised from Fox et al. (1995) and our
209   new data.

Palate

211   Fox et al. (1995) admitted that the palatal bones of *Cladarosymblema* were not well known. Those
212   authors managed to piece together a composite reconstruction of the parasphenoid from several
213   specimens, but failed to recover complete pterygoid bones. The palatoquadrate complex is
214   preserved within the holotype and revealed in the scan data (Fig. 1). It is thin and forms a shallow
215   concavity dorsally. Its margins flex upwards where it abuts the lateral sphenoid portion of the
216   braincase (basipterygoid), the anterolateral face of the oticoccipital and the quadrate articulation
217   posteriorly. In contrast, the posterolateral corner bears a more downturned, smoother edge.
218   Anteriorly the pterygoids are generally flat in the dorsoventral plane, but their posterior half is
219   flexed more into the sagittal plane. In ventral view the right pterygoid bears a longitudinal ridge
220   separating its medial and lateral portions (Fig. 1d).

Mandible

222   Fox et al. (1995) were unable to confidently recognise sutures between dermal bones on the
223   mandible on *Cladarosymblema*, despite attempting this by using radiographic images. The holotype
224   fails to illuminate this further as much of the dermal bone has eroded. These boundaries were also
225   noted to be difficult to ascertain in *Askerichthys* (Borgen & Nakrem 2016) so this may be a feature
226   common among megalichthyids. As discussed in the original description by Fox et al. (1995), we can
227   herein confirm that there is no oral branch of the canal in the surangular and that the anterior
228   mandibular fossa received the vomerine tusk. The anterior coronoid is longer than the following
229   two, and there are three tusks present (Fig. 2). *Askerichthys* (and also probably *Ectosteorhachis*) are
230   known to possess just two (Borgen & Nakrem 2016; Thomson 1964). The parasymphysial tooth plate
231   is known to vary in shape between specimens, that in the holotype forms an elongate triangle
232   covered in small denticles (Fig. 2b-c).

Endocranium and Endocast

234   The new data generated herein permit the reconstruction of the virtual cranial endocast for this
235   taxon. Comparisons are made principally with other tetrapodomorphs for which a full endocast is
236   known, namely *Gogonasus* (Holland 2014), *Ectosteorhachis* and *Megalichthys* (Romer 1937), and
237   *Eusthenopteron* ~~Jarvik 1955~~ (Stensiö 1963). Other Palaeozoic sarcopterygians with complete

238   endocasts depicted in the literature include the dipnomorph *Youngolepis* (Chang 1982), the
239   onychodont *Qingmenodus* (Lu et al. 2016), the coelacanth *Diplocercides* (Stensiö 1963), several
240   lungfish taxa (Challands 2015; Clement & Ahlberg 2014; Clement et al. 2016; Henderson & Challands
241   2018; Miles 1977; Säve-Söderbergh 1952) and the aïstopod *Lethiscus* (Pardo et al. 2017).
242   Furthermore, partial yet still informative endocasts are known from the stem-tetrapod *Tungsenia*
243   (Lu et al. 2012), porolepiforms *Powichthys* (Clément & Ahlberg 2010) and *Glyptolepis* (Stensiö 1963),
244   the tetrapodomorph *Spodichthys* (Snitting 2008) and *Ichthyostega* (Clack et al. 2003).

245   The endocast of the holotype (QMF 21082) measures just over 50 mm long from the base of the
246   olfactory tracts to the vagus nerve (n.X), and 30 mm at its widest point across the labyrinths (Fig. 3a).
247   As the holotype has suffered some dorsoventral compression during preservation, fine details such
248   as the morphology of the semicircular canals has been lost. Despite this, the gross morphology of
249   the endocast can for the first time be revealed in *Cladarosymblema*. The isolated ethmosphenoid
250   (QMF 21083) is well-preserved and has only a little localised crushing internally, and so revealed the
251   olfactory and hypophyseal regions particularly well (Fig. 4d-h).

252   The overall proportions of the endocast in *Cladarosymblema* are similar to those in *Youngolepis*
253   *Gogonasus*, *Megalichthys* and *Eusthenopteron* in having widely separated nasal capsules on long
254   olfactory tracts, a narrow forebrain, but broad mid- and hindbrain regions. The contrasts starkly with
255   the presumed plesiomorphic condition in *Tungsenia* which bears short olfactory tracts and a bulbous
256   telencephalic region.

257   The nasal capsules are large and rounded with a diameter close to 10 mm, and open ventrally. Their
258   posteromesial corners open into wide olfactory tracts that are 15 mm long and diverge from each
259   other at 50°. The canals for the orbitonasal vein are large and exit the nasal capsules
260   posterolaterally. Several bony tubules project into the medial rostral space from the olfactory tracts
261   which may have housed the anterior cerebral vein, palatine artery or a ramus of maxillaris nV_2.

262   The telencephalic region is short and low, without any obvious ventral expansion as is common in
263   lungfish (Clement & Ahlberg 2014). Two large canals for the optic nerves exit the cranial cavity
264   laterally marking the anterior extent of the telencephalic region. In contrast, the diencephalic region
265   is both longer and taller, although of comparable width to the telencephalon. A small dorsal
266   protrusion represents a small pineal eminence, seemingly smaller than those in *Eusthenopteron* and
267   *Gogonasus*. In contrast, the hypophyseal fossa is large. The buccohypophyseal duct opens through a
268   large circular aperture ventrally. Two dorsal-most small canals projecting anteriorly from the
269   hypophyseal region likely housed the ophthalmic arteries, in line with but medial to those is a single
270   small canal that might have housed the internal carotid artery. Below this, two slightly larger canals
271   would have carried the palatine arteries. On the left side of the QMF 21083 on the posterior half of
272   the hypophyseal region is a single small canal that could have carried the pituitary vein.

273   The mesencephalic region of the endocast is considerably broader than the preceding forebrain.
274   Midway up on the midbrain wall is a canal for the trigeminal nerve (n.V), likely housing both the
275   maxillary and mandibular branches. The rhombencephalic region is very slightly wider than the
276   midbrain, broadening gently towards the labyrinths as in *Megalichthys*, and in contrast to
277   *Gogonasus* which is reconstructed as being narrower in this area. Canals for the vagus nerve (n.X)
278   are visible exiting the cranial cavity posteriorly. Two oval-shaped eminences on the dorsal part of the
279   myelencephalon represent the supraoptic cavities, and the cranial cavity extends a further 14 mm
280   towards and into the intracranial joint.

281　Although the specimen has been flattened and undergone some crushing, the origin point of the
282　posterior semicircular canals can be identified, so together with the lateral extent of the labyrinth, a
283　rough outline of the vestibular system can be inferred. It is not known how large any utricular recess
284　might have been, but the saccular pouches form tear-drop-shaped outlines in ventral view, with
285　rounded anterior margins tapering posteriorly.

286　The notochordal canal is broad and probably extended as far forward as to be level with the
287　midbrain, although the bounding bone is not preserved well anteriorly.

288　**Hyoid and Branchial Skeleton**

289　We are now able to describe most of the elements of the hyoid arch and branchial skeleton as
290　preserved *in situ* within the holotype. The hyomandibular and supposed 'urohyals' were described
291　by Fox et al. (1995), but we can now correct their identification of the 'urohyal' in Figure 43A-D as
292　more likely being median fin basal elements. The urohyal revealed in our articulated specimen is a
293　much-elongated bone with a very wide anterior articulation surface for meeting the basibranchial.

294　One complete right hypohyal (and a partial left hypophyal, not figured) sit anterolateral to the
295　basibranchial (Fig. 4). The hypohyal bears a ball-shaped protuberance proximally for articulation with
296　the anterolateral articular facet of the basibranchial. The distal portion is broadly flared and its
297　shape is similar to those in other tetrapodomorphs, such as *Tiktaalik* (Downs et al. 2008) and
298　*Eusthenopteron* (Jarvik 1954; Jarvik 1980). It bears a strong ridge running proximodistally along its
299　dorsal surface, as also seen in *Holoptychius* (Cloutier & Schultze 1996).

300　The right ceratohyal (Fig. 4d) a large, mostly flat tear-drop shaped bone, with a smoothed curved
301　anterior margin. It is marked by a large notch in its posterolateral corner for ligamentous
302　attachment. Its shape differs somewhat from those in *Gogonasus* (Long et al. 1997), *Tiktaalik*
303　(Downs et al. 2008) and *Medoevia* (Lebedev 1995), which have more elongate and narrower
304　ceratohyals, instead it is more reminiscent of the broader bones found in *Glyptolepis* (Jarvik 1972).

305　The basibranchial (Fig. 4c) is similar to those in *Tiktaalik* (Downs et al. 2008), *Gogonasus* (Long et al.
306　1997), *Medoevia* (Lebedev 1995) and *Mandageria* (Johanson & Ahlberg 1997). It forms a slightly
307　elongated heptagonal shape in dorsal view. The basibranchial is clearly split (appears to be a natural
308　margin) into two transverse halves demarcated by mesiolateral angles that separate it into anterior
309　and posterior portions of similar size. The three lateral and posterior margins are scalloped for
310　articulation with the hypobranchials on each side and the hypohyals anterolaterally.

311　There are four hypobranchials preserved on the right-hand side (Fig. 4c). The first articulates with
312　the anterior portion of the basibranchial, while the second and third articulate with the posterior
313　half of the basibranchial. The fourth hypobranchial, considerably smaller than the other three, is
314　preserved in articulation with the posterior section of the third hypobranchial, as in common among
315　sarcopterygians. The hypobranchials are more elongate than the stouter bones in *Tiktaalik* (Downs
316　et al. 2008) being more similar to those in *Medoevia* (Lebedev 1995). The first hypobranchial has a
317　broader anterior margin, and its medial margin is curved more strongly, while the second and third
318　have more or less parallel edges and narrower anterior edges. The fourth hypobranchial is about half
319　the size of the preceding three hypobranchials, but with a similar shape to the third hypobranchial
320　with which it articulates.

321　In ventral view, a sublingual rod and urohyal are preserved underneath the basibranchial in natural
322　articulation (Fig. 4d). The sublingual rod is an elongate and narrow bone that tapers slightly

323   anteriorly. It is considerably shorter than that in *Eusthenopteron* (Jarvik 1980) but of similar length
324   to that in *Medoevia* (Lebedev 1995). The urohyal is long and rod-like but does not appear to
325   bifurcate posteriorly nor bear a large posterior flange. In this way the urohyal is similar to that in
326   *Gogonasus* (Long et al. 1997).

327   Four ceratobranchials are preserved on both left and right sides of the specimen. Three are long and
328   curved measuring about 45 mm in length, but the fourth is highly reduced and lacks a grooved
329   portion. These are currently under more detailed study in another work currently in preparation by
330   the authors.

331   The general shape of the hyomandibular (Fig. 4c) is similar to *Eusthenopteron* (Jarvik 1980), although
332   it is not so strongly curved in *Cladarosymblema*. It appears to have been a completely ossified bone,
333   more similar to that in *Gogonasus* (Long et al. 1997) and unlike the unfinished one in *Tiktaalik*
334   (Downs et al. 2008). Its proximal extremity is double-headed and its distal end contacts the mesial
335   face of a submandibular bone via its opercular process. There is a large opening between the lateral
336   and medial margins of the proximal portion that would have allowed passage of the hyomandibular
337   canal.

338   **Pectoral girdle and fin**

339   The pectoral girdle of *Cladarosymblema* was described by Fox et al. (1995) from several partial or
340   broken bones. While we fail to identify a supracleithrum in the scan of the holotype, we do see both
341   clavicles, cleithra and anocleithra well-preserved (Fig. 5a-f). Previously, the anocleithra were
342   represented by just two fragments but we have recovered both complete bones. The anterior
343   process is about 12 mm in length and sharply pointed on the left bone, but more rounded on the
344   right-hand side. The posterior flange of the anocleithra is smooth and flat, and measures over 30
345   mm in length.

346   Similarly, Fox et al. (1995) did not have complete cleithra, but we can now herein describe and
347   illustrate these bones. The cleithra are robust bones with a sizeable branchial lamina. Its external
348   surface is roughened with ornament. It has a pointed anterior margin for overlap with the clavicles,
349   but a broad and blunt posterior margin. Although there are some cracks present through this region
350   of the specimen, we can confirm that the cleithrum was a single bone, *contra* Thomson & Rackoff
351   (1974).

352   As described by Fox et al. (1995), the clavicles are indeed about half the size of the cleithra and
353   twisted some 40° in orientation. Again, the right-hand side bone is better preserved than the left. Its
354   ventral edge is smoothly rounded, while the dorsal surface bears a thickening. The clavicle bears a
355   long ascending process for articulation with the cleithrum. In addition, there is a small, ovoid bone
356   sitting dorsally above the intersection of the clavicles, interpreted as an unornamented interclavicle,
357   the first time this bone has been identified in this taxon.

358   Fox et al. (1995) stated that the scapulocoracoid and its attachment area is larger in
359   *Cladarosymblema* than in other osteolepiforms, but that in the holotype is not as extensive as the
360   specimen described and illustrated by those authors. Conversely, the scapulocoracoid in fact
361   appears to be smaller and protruding less than those in *Eusthenopteron* (Jarvik 1980), *Megalichthys*
362   (Andrews & Westoll 1970), and *Medoevia* (Lebedev 1995).

363   In their original preparation and description of the holotype, Fox et al. (1995) attempted to excavate
364   the axial skeleton of the left fin but did not find it, concluding that it must have been poorly ossified.

365 Radiographs show an outline of some large metaptyerygial elements of the pectoral fin but scan
366 artefacts from the metallic wire supporting the perimeter of the fin limit our potential to find any
367 evidence of any ossified pectoral mesomeres in the remaining pectoral fin area of the holotype. In
368 any case, we conclude that these may have even been cartilaginous in *Cladarosymblema*.

369 **Axial skeleton**

370 As Fox et al. (1995) described in the original description, vertebral ring centra are preserved that are
371 about 11-12 mm in notochordal diameter, and open dorsally. However, those authors fail to figure
372 or describe the neural arches. The neural arches (Fig. 5g,i,k) are similar to those figured for
373 *Eusthenopteron* (Andrews & Westoll 1970a) and as is common, usually found slightly disarticulated
374 from their associated ring centra (Fig. 5h,j,l). The two halves of the neural arch join dorsally to form a
375 neural spine, and these are angled about 35 degrees posteriorly from the vertical plane. The neural
376 arches are flat bones with only a very slight tapering at their dorsal tips.

377 The elements originally identified by Fox et al. (1995) as two isolated urohyals (QMF 26574 and QMF
378 26573) are reidentified as proximal basal plate of the second dorsal and/or anal fins. The proximal
379 end is narrow, whereas the distal end is approximately three times longer showing three articular
380 facets for the distal radials. The morphology of the proximal basal plate of *Cladarosymblema* is fairly
381 similar to that observed in *Eusthenopteron foordi* (Andrews and Westoll 1970, text-fig. 25, 26, 28).

382

383

384 **PHYLOGENETIC RESULTS**

385 Interrelationships among nine species of megalichthyids and the phylogenetic position of
386 megalichthyid species among tetrapodomorphs were analysed using a modified version of the
387 tetrapodomorph matrix used by Cloutier et al. (2020). From the original *Cladarosymblema* coding in
388 Cloutier et al.'s (2020) phylogenetic matrix, an additional ten characters (72-74, 110-112, 133, 148,
389 190, 197) were coded based on our new anatomical study. The parsimony analysis (heuristic search)
390 of the complete data matrix (48 taxa, 206 characters) gave 24 948 equally parsimonious trees at 494
391 steps [consistency index = 0.484, retention index = 0.759]. The general tetrapodomorph topology is
392 similar to the one obtained by Cloutier et al. (2020). The monophyly of megalichthyids has been
393 recovered in the three consensus trees (strict, Adams, 50% majority), the results from the 50%
394 majority-rule tree is shown in Figure 6. Megalichthyids are considered the sister-group to
395 canowindrids. "Osteolepidids" (represented by *Osteolepis, Gyroptychius, Medoevia,* and *Gogonasus*)
396 form a grade leading to the clade megalichthyids + canowindrids; the inclusion of additional
397 megalichthyids in our analysis regrouped "osteolepidids" at the base of the clade megalichthyids +
398 canowindrids.

399 *Palatinichthys laticeps* is the sister-group of the remaining megalichthyids in the three consensus
400 trees, followed by *Megalichthys hibberti*. In the 50% majority (Fig. 6a) and strict consensus trees
401 *Cladarosymblema* forms part of a polytomy including *Sengoerichthys, Megalichthyis laticeps* and *M.*
402 *mullisoni* and [*Askerichthys + Mahalalepis*]. The Adams consensus tree suggests that two of the most
403 incomplete megalichthyids are responsible for the internal polytomies: *Sengoerichthys ottoman* (164
404 unscored and 3 illogical), and *Megalichthys laticeps* (161 unscored and 6 illogical).

405   The deletion of the most incomplete megalichthyids [i.e., species with more than 40% of unscored
406   characters: *Mahalalepis resima* (173 unscored and 0 illogical), *Palatinichthys laticeps* (135 unscored
407   and 5 illogical), *Askerichthys heintzi* (130 unscored and 4 illogical), and *Megalichthys mullisoni* (92
408   unscored and 6 illogical)] did not modify the position of the remaining megalichthyids on the tree
409   but reduced considerably both the number of step (471) and the number of equally parsimonious
410   trees (702). An analysis on 44 taxa including a subset of megalichthyids using the best-known species
411   of *Megalichthys* (i.e., *M. hibberti*) and excluding the two most incomplete megalichthyids (i.e.,
412   *Sengoerichthys ottoman* and *Mahalalepis resima*) provide better resolved megalichthyid
413   interrelationships of 481 steps and 648 equally parsimonious trees (Fig. 6b). The ~~tree~~ consensus
414   trees recovered the following topology: [*Palatinichthys* [*Megalichthys* [*Askerichthys*, *Ectosteorhachis*,
415   *Cladarosymblema*]]].

416   The monophyly of the megalichthyids is supported by the presence of a long medioventral process
417   of the premaxilla (char. 203), the antero-posterior relationships between the lateral rostral and the
418   anterior tectal relative to the external nostril (character 5; this character could also be phrased as
419   the vertical suture between these two dermal bones at the level of the external nostril). The
420   presence of the anterolateral process of the supratemporal (char. 206) is also shared by most
421   megalichthyids with the exception of *Palatinichthys*. However, this process is also known in
422   *Eusthenopteron, Gyroptychius* and *Kenichthys*. The absence of a pineal foramen (char. 21)
423   characterizes the megalichthyids but is also absent in most of our outgroups.

424

425

DISCUSSION

Systematic Implications

428   *Cladarosymblema* is significant as the only megalichthyid taxon described from Australia, and along
429   with *Mahalalepis*, one of only two known from Gondwana. Previously unseen morphological details
430   of the cranial endocast, palate, hyoid and branchial skeleton, pectoral girdle and axial skeleton of
431   *Cladarosymblema* are now elucidated, with additional features confirmed or updated from Fox et
432   al.'s (1995) description. These new data, with additional codings from *Mahalalepis*, and the inclusion
433   of nine megalichthyid species in the parsimony analysis, enabled megalichthyid interrelationships to
434   be reanalysed, with the monophyly of the family confirmed. A full lateral reconstruction of the head
435   of *Cladarosymblema* is shown in Figure 7.

436   *Revised Diagnosis of the Family Megalichthyidae:* Stem-tetrapodomorph fishes at a node higher ~~then~~
437   *Osteolepis* and lower than *Eusthenopteron* which have the following characters: small semi-circular
438   shaped lateral rostral and posterior tectal forming the external nostril dorso-ventrally; premaxilla
439   bearing a well-developed posterior process and tusk that interrupts or lies lingual to the premaxillary
440   marginal tooth row; contact between the subopercular and ~~second~~ submandibular; and a distinct
441   supratemporal bone with an anterolateral process lacking cosmine cover.

442   With respect to the phylogenetic status of the Megalichthyidae, Schultze (1974) first identified the
443   specificity of megalichthyids based on the development of the external nares as slit-like openings,
444   partially enclosed by a small posterior tectal bone, and the presence of an intermaxillary process
445   with teeth on the premaxillae.

446   Seven characters were originally used by Young et al. (1992) to diagnose the Megalichthyidae (our
447   numbering of characters): (Y+1) elongate or slit-like external naris (Y+2) partly enclosed by a
448   posterior tectal bone, (Y+3) presence of an interpremaxillary process with teeth on the premaxilla,
449   (Y+4) short and broad vomers with a strong mesial process, (Y+5) closed pineal foramen, (Y+6)
450   parietals (their "frontal bones") notched for the posterior nasals, and (Y+7) well-developed lacrimal
451   notch.

452   Using an additional 15 features, Fox et al. (1995) provided a general diagnosis for the
453   Megalichthyidae that was not intended to be a phylogenetic diagnosis, but rather a general
454   differentiation from other osteolepiform families. Among Fox et al.'s (1995) features that had not
455   been listed by Young et al. (1992), new potential synapomorphies were listed (our numbering of
456   characters): (F+1) separate bones dorsal and ventral of the narial opening, (F+2) two suboperculars
457   both abutting the posterior-most submandibulars, (F+3) posterior endocranial wall of
458   trigeminofacialis chamber approximately transverse, (F+4) strong symphysial tusk on dentary and
459   teeth reduced or absent in front of it.

460   While assessing the phylogenetic position of *Litoptychius*, Coates & Friedman (2010) mentioned that
461   it shares synapomorphies with megalichthyids including some new neurocranial features (our
462   numbering of characters): (C&F1) ethmoid articulation for palatoquadrate extends anterior to
463   postnasal wall; (C&F2) nerves II and III exit through common foramen; (C&F3) posteriorly extensive
464   basicranial fenestra; (C&F4) otico-occipital fissure absent; and (C&F5) articular surface of quadrate
465   located above ventral margin of the palatoquadrate.

466   In their exhaustive study on "osteolepiforms", Borgen and Nakrem (2016) reviewed features
467   previously used to diagnose the Megalichthyidae to select 11 of which they identified either as
468   indicative, necessary or sufficient character to diagnose the group. Among the unambiguous
469   necessary and sufficient characters, they listed five of their 11 characters (their numbering of
470   characters): (B&N1) anterior palatal dental morphology with the presence of anterior premaxillary
471   tusks (in row or posterior to small, same size marginal premaxillary teeth; their "morphotype C and
472   D", respectively) in combination with a cosmine covered surface of the cranium, (B&N4) the
473   presence of a branch from the supraorbital sensory canal running towards the anterior tectal (their
474   "postnarial"), (B&N6) a distinct cosmine-less anterior supratemporal (their "intertemporal") process
475   situated mesial to the opening of the sensory canal (i.e., the supraorbital canal), and (B&N10) a
476   posterior contact between the second submandibular and subopercular and first submandibular.

477   Based on the revision provided by Borgen and Nakrem (2016), Downs and Daeschler (2020) reduced
478   the diagnosis to just four synapomorphies (their numbering of characters): (D&D1) presence of a
479   cosmine cover on dermal bones, (D&D2) a premaxillary tusk that interrupts or lies lingual to the
480   premaxillary marginal tooth row (from Young et al. 1992), (D&D3) contact between the subopercular
481   and the second submandibular bones (from Fox et al. 1995), and (D&D4) a distinct rostral process of
482   the supratemporal that is without cosmine cover.

483   Most of these megalichthyid features and synapormophies have already been discussed by Fox et al.
484   (1995), Borgen and Nakrem (2016) and Downs and Daeschler (2020). However, additional comments
485   on some of the characters listed above are provided herein. Since Fox et al. (1995), the organization
486   of the bones forming the external naris (F+1) has been recognized as a distinctive feature of
487   megalichthyids. The narial region of megalichthyids in comparison to other "osteolepiforms"

488   necessitates further investigation in order to quantify the size of the naris (Y+1), the relative size of

489   narial surrounding bones (Y+2; char. 204, 205), and the precise trajectory of the sensory canals

490   (B&N4). Although, megalichthyid external nares seem to be elongated (Y+1) one would have to

491   quantify the shape of the external naris among tetrapodomorphs to properly evaluate this character.

492   The cheek regions of megalichthyids is poorly known, although it might represent some diagnostic

493   features (e.g., shape of the squamosal, shape and height of the dorsal margin of the maxilla, size and

494   orientation of the preopercular) it is difficult at the moment to use these cheek characters as

495   diagnostic of the group. The presence of an enlarged anterior tooth on premaxilla (Y+3 in part, B&N1

496   in part, D&D2; char. 76, 187) and the presence of a long medioventral process of the premaxilla

497   (char. 203) are present in megalichthyids but the enlarged anterior tooth of the premaxilla is also

498   present in rhizodonts and some "osteolepididids". The absence of the pineal foramen (Y+5; char. 21)

499   was also reported in most of the outgroups used in our analysis; it might well be a plesiomorphic

500   condition or a homoplastic feature among osteichthyans (Janvier et al. 2007). Bjerring (1972)

501   suggested that the anterolateral process of the supratemporal (his "frontodermosphenotic process

502   of the intertemporal" and "area of intertemporal overlapped by dermosphenotic") showing a

503   complex articular structure for the parietal and the intertemporal is characteristic of the

504   Megalichthyidae (Janvier et al. 2007). The presence of the anterolateral process of the

505   supratemporal (B&N6 in part, D&D4; char. 206) is shared by most megalichthyids with the exception

506   of *Palatinichthys*. However, an anterolateral process on the supratemporal is also present in

507   *Eusthenopteron, Eusthenodon, Gyroptychius* and *Kenichthys*. The proportion of the vomer (char. 61)

508   as well as the presence of an anteromedial process of the vomer (Y+4 in part; char. 62) should be

509   quantified properly in order to be compared among tetrapodomorphs. The vomers are much

510   broader than long in megalichthyids and some "osteolepididids" and this is also accurate for the

511   presence of the anteromedial process of the vomer.

512   Concerning the phylogenetic intrarelationships of the Megalichthyidae, taxa previously considered

513   by some researchers (Downs & Daeschler 2020; Witzmann & Schoch 2012) to hold dubious affinities

514   (such as *Mahalalepis, Palatinichthys* and *Sengoerichthys*) are confirmed as megalichthyid taxa in our

515   analysis (Fig. 6).

516   Previous phylogenetic analyses included three (Ahlberg & Johanson 1998; Cloutier et al. 2020;

517   Johanson & Ahlberg 2001; Simões & Pierce 2021; Zhu & Ahlberg 2004; Zhu et al. 2017), four (Young

518   et al. 1992), or five megalichthyids (Witzmann & Schoch 2012). Thus, our phylogenetic analysis

519   contains the largest megalichthyid diversity included in a phylogenetic analysis with nine species.

520   Megalichthyid intrarelationships recovered from our analysis somewhat resemble that of Witzmann

521   & Schoch (2012) in nesting *Palatinichthys* and *Ectosteorhachis* close together, and *Cladarosymblema*

522   close to *Sengoerichthys*. Although the position of *Megalichthys* differs. We propose that this taxon is

523   unstable, influencing the topology whether considered as one taxon or split into species, and is likely

524   paraphyletic. Future analyses will have to include all anatomical features that have been previously

525   discussed in the literature with respect to the phylogenetic status of megalichthyid family, genera

526   and species.

527

528

529

Palaeoneurology

530

531   Increasing access to scanning technologies such as synchrotron, neutron and micro- computed
532   tomography (µCT) is advancing palaeontology and in particular the field of "palaeoneurology", yet
533   still very few tetrapodomorph endocasts are known. Consequently, little is understood about
534   changes to brain morphology during this vital period of evolution approaching the fish-tetrapod
535   transition. In particular, the internal space within the braincase, the 'endocast' will prove valuable
536   for developing hypotheses about neural evolution within members on the tetrapodomorph stem. In
537   the absence of (exceedingly rare) preserved brains, evidence from the extant phylogenetic bracket
538   (lobe-finned fish and amphibians) suggests that we may still be able to make some inferences about
539   the size of certain brain regions from the shape of the endocast alone (Challands et al. 2020;
540   Clement et al. 2021; Clement et al. 2015).

541   *Megalichthys* (Romer 1937) and *Eusthenopteron* (Stensiö 1963) had their endocasts manually
542   reconstructed in detail via Sollas' painstaking and destructive grinding method popularized by the
543   Stockholm School (Schultze 2009). Partial virtual endocasts (ethmosphenoids) have been described
544   more recently of the stem-tetrapod, *Tungsenia* (Lu et al. 2012), and the 'osteolepiform' *Spodichthys*
545   (Snitting 2008) from CT data. To date, *Gogonasus* (Holland 2014) remains the only tetrapodomorph
546   for which its full braincase has been investigated via tomographic data, but a full endocast was
547   neither figured nor described.

548   With respect to early tetrapod endocasts, a small section of an eroded *Ichthyostega* braincase was
549   figured in Clack et al. (2003) illustrating a portion of the oticoccipital, Pardo et al. (2017) figured an
550   endocast from the Early Carboniferous aïstopod, *Lethiscus*, and the endocast was described from the
551   Permian temnospondyl, *Eryops* (Dempster 1935).

552   Thus, the description of the endocast of *Cladarosymblema* herein provides a valuable addition
553   enabling new insight into the neurobiology of the tetrapod stem group. *Cladarosymblema* and
554   *Eusthenopteron* have olfactory tracts shorter and broader than those in *Megalichthys* and
555   *Gogonasus*. The nasal capsules are widely separated from each other and positioned on long
556   olfactory canals, and the forebrain is narrow in all figured tetrapodomorphs (except for *Tungsenia*),
557   with the mid and hindbrain regions are broader and appear relatively conserved across taxa. While it
558   is problematic to make broad generalisations based on such a small sample, it is striking to note far
559   greater morphological diversity appears to exist in the endocasts of a comparable group, Palaeozoic
560   lungfish, compared to all known stem tetrapods (Clement et al. under review).

561   The hypophyseal fossa is another region of the braincase that bears further consideration here. The
562   orientation of the hypophyseal region varies among taxa with *Tungsenia* (Lu et al. 2012),
563   *Diplocercides* (Stensiö 1963), *Youngolepis* (Chang 1982) and most lungfish (Clement et al. 2016)
564   having small, ventrally-directed hypophyseal fossae. In contrast, *Eusthenopteron* (Stensiö 1963),
565   *Spodichthys* (Snitting 2008), *Gogonasus* (Holland 2014), *Qingmenodus* (Lu et al. 2016) and several
566   Palaeozoic actinopterygians (Giles & Friedman 2014) have thinner and narrower ones that extend
567   considerably further ventrally. In *Cladarosymblema* and *Megalichthys* the hypophyseal fossa is a
568   more robust structure, extending ventrally from the cranial cavity but with a sizeable anteriorly-
569   projecting lobe. *Diplocercides* and *Youngolepis* also have significant lobes on their hypophyseal
570   fossae, but these are oriented posteriorly in those taxa.

571 The anteriorly-oriented space in megalichthyids may potentially accommodate the pars tuberalis as
572 hypothesised for *Tungsenia* and *Glyptolepis* (Lu et al. 2012). The pars tuberalis is part of the pituitary
573 gland and is present in all tetrapods but particularly well developed in mammals (Kardong 2006). It
574 is thought to play a role in sensing photoperiod and was taken as supporting evidence that some
575 brain modifications in stem tetrapods for an increasingly terrestrial lifestyle had appeared as long
576 ago as the Early Devonian (Lu et al. 2012). However, the pars tuberalis, when present, is only a very
577 small upgrowth around the stalk of the infundibulum and may potentially be too small to be
578 reflected in some endocasts. In fact, it is not recognisable in a recent investigation of some extant
579 salamander (Challands et al. 2020) nor frog and caecilian endocasts (Clement et al. 2021).

580 We suggest that the enlarged anterior lobe of the hypophyseal region as seen in *Cladarosymblema* is
581 most likely reflecting an expanded pars distalis. The pars distalis consists of secretory cells and
582 comprises the bulk of the adenohypophysis ("anterior lobe" of the pituitary) which plays a large role
583 in the production of numerous hormones (Romer & Parsons 1985). This is not to say that animals
584 lacking a pars tuberalis were not sensitive to photoperiod, as even extant fishes which lack a pars
585 tuberalis (chondrichthyans and teleosts) can, for example, sense seasonal changes in day length via
586 their saccus vasculosus instead (Nakane et al. 2013).

587
588

589 **CONCLUSIONS**

590 Synchrotron and μCT of two well-preserved 3D specimens of *Cladarosymblema* confirm and update
591 the original description of this taxon, in addition to revealing never-before-seen details of its
592 anatomy, enabling a more comprehensive understanding of the only Australian megalichthyid. This
593 work highlights the value of tomography to supplement traditional preparation and descriptions of
594 key fossil specimens. New details -particularly from ~~that of~~ the palatoquadrate complex, hyoid and
595 branchial arches, pectoral girdle, and axial skeletons- greatly increase our understanding of this
596 "osteolepidid-grade" tetrapodomorph, boosting our knowledge of the total morphological diversity
597 within this group. In addition, while several cranial endocasts are known from manual
598 reconstructions or isolated ethmosphenoids, *Cladarosymblema* enables the reconstruction and
599 visualisation of the first full virtual (from tomographic data) cranial endocast of a tetrapod-like fish,
600 enabling greater insight into their neurobiological condition, including characteristics of note such as
601 the size and shape of the pituitary gland. A new phylogenetic analysis confirms the monophyly of the
602 Megalichthyidae, which includes seven genera (*Askerichthys, Cladarosymblema, Ectosteorhachis,*
603 *Mahalalepis, Megalichthys* spp.*, Palatinichthys* and *Sengoerichthys*), and their position within
604 Tetrapodomorpha more broadly. An updated familial diagnosis is provided.

605
606

607 **Funding Sources**

623

Figure Captions

625 **Figure 1. Micro-CT 3D rendering (58 μm pixel size) of dermal skull and braincase of**
626 ***Cladarosymblema* (QMF 21082).** A, skull in dorsal view showing placement of bones on holotype; B,
627 braincase in ventral view; dermal skull bones, braincase and palatal bones in C, dorsal and D, ventral
628 view; E, skull and cheek in right lateral view.

629 **Figure 2. Micro-CT 3D rendering (58 μm pixel size) of mandible and submandibular bones of**
630 ***Cladarosymblema* (QMF 21082).** A, mandibular bones in ventral view showing placement of bones
631 on holotype; mandible in B, dorsal; C, lingual; and D, labial view.

632 **Figure 3. Micro-CT 3D (58 μm pixel size) and synchrotron rendering (12 μm pixel size) of cranial**
633 **endocast and sensory lines of *Cladarosymblema* (QMF 21082).** A, dorsal; b, ventral; and C, left
634 lateral view; QMF 21083 in D,E, dorsal view; F,G, ventral view; H, left lateral view showing zoomed in
635 hypophysial fossa region.

636 **Figure 4. Micro-CT 3D rendering (58 μm pixel size) of hyoid and branchial skeleton of**
637 ***Cladarosymblema* (QMF 21082).** A, skull in dorsal view showing placement of bones on holotype; B,
638 in ventral view; C,D, full hyoid and basibranchial skeleton including ceratobranchials as preserved *in*
639 *situ*.

640 **Figure 5. Micro-CT 3D rendering (58 μm pixel size) of pectoral and axial elements of**
641 ***Cladarosymblema* (QMF 21082).** A, ventral view, and B, in dorsal view, showing placement of bones
642 on holotype; pectoral girdle in C, dorsal view; and D, ventral view; E, F, anocleithra in alternate
643 views; and neural arches in G, lateral; I, dorsal; K, ventral view; ring centra in H, lateral; J, dorsal; L,
644 ventral view.

645 **Figure 6. Parsimony analyses.** A, 50% majority-rule consensus tree from parsimony analysis with
646 inclusion of all taxa showing monophyly of the Megalichthyidae; B, Canowindrid + Megalichthyid
647 sub-set with most incomplete taxa excluded (*Mahalalepis, M. mullisoni, M. laticeps, Sengoerichthys*)
648 provides greater resolution of megalichthyid phylogeny. Image silhouettes are authors own
649 (elpistostegalids, rhizodonts, megalichthyid) or from PhyloPic http://phylopic.org/ (*Ichthyostega*,
650 Scott Hartman; *Eusthenopteron* & *Gogonasus*, Michael Keesey).

651   **Figure 7. Lateral head reconstruction of *Cladarosymblema.*** Compiled from Fox et al. (1995) and
652   new data presented herein. Colour-coded as follows: dermal skull roof (dark blue), cheek (light blue),
653   lower jaw (pale green), opercular series (purple), and pectoral (dark green). Bones marked with "?"
654   remain unknown in this taxon.

655   **SI-Figure 1.** Tomographic data example slice of A,B, holotype QMF 20182 (Micro-CT 3D rendering,
656   scan performed at 58 µm pixel size), and C,D, QMF 21083 (synchrotron-CT rendering, scan
657   performed at 12 µm pixel size); E, X-ray image of holotype QMF 20182 showing total field of view
658   and X-ray attenuation.

659

660

661   # References

662   Agassiz JLR. 1835. On the fossil fishes of Scotland. *Report of the Fourth Meeting of the British*
663   *Association for the Advancement of Science*. Edinburgh in 1834: John Murray, London, 646–
664   648.
665   Ahlberg PE, and Johanson Z. 1998. Osteolepiforms and the ancestory of tetrapods. *Nature* 395:792-
666   794.
667   Andrews SM, and Westoll TS. 1970a. The postcranial skeleton of *Eusthenopteron foordi* Whiteaves.
668   *Transactions of the Royal Society of Edinburgh* 68:207-329.
669   Andrews SM, and Westoll TS. 1970b. The postcranial skeleton of Rhipidistian fishes excluding
670   *Eusthenopteron*. *Transactions of the Royal Society of Edinburgh* 68:489.
671   Bjerring HC. 1972. Morphological observations on the exoskeletal skull roof of an osteolepiform
672   from the Carboniferous of Scotland. *Acta Zoologica* 53:73-92.
673   Borgen UJ, and Nakrem HA. 2016. Morphology, phylogeny and taxonomy of osteolepiform fish.
674   *Lethaia*.
675   Challands TJ. 2015. The cranial endocast of the Middle Devonian dipnoan *Dipterus valenciennesi* and
676   a fossilised dipnoan otoconal mass. *Papers in Palaeontology* 1:289-317.
677   Challands TJ, Pardo JD, and Clement AM. 2020. Mandibular musculature constrains brain-endocast
678   disparity between sarcopterygians. *Royal Society Open Science* 7:1-20.
679   Chang MM. 1982. The braincase of *Youngolepis*, a Lower Devonian crossopterygian from Yunnan,
680   south-western China PhD. University of Stockholm and Section of Palaeozoology, Swedish
681   Museum of Natural History.
682   Clack JA, Ahlberg PE, Finney SM, Dominguez Alonso P, Robinson J, and Ketcham RA. 2003. A uniquely
683   specialized ear in a very early tetrapod. *Nature* 425:65-69.
684   Clement AM, and Ahlberg PE. 2014. The first virtual cranial endocast of a lungfish (Sarcopterygii:
685   Dipnoi). *PloS One* 9:e113898. 10.1371/journal.pone.0113898
686   Clement AM, Challands TJ, Cloutier R, Houle L, Ahlberg PE, Collin S, and Long JA. under review.
687   Morphometric Analysis of Lungfish Endocasts Elucidates Early Dipnoan Palaeoneurological
688   Evolution. *eLife*.
689   Clement AM, Challands TJ, Long JA, and Ahlberg PE. 2016. The cranial endocast of *Dipnorhynchus*
690   *sussmilchi* (Sarcopterygii: Dipnoi) and the interrelationships of stem-group lungfishes. *PeerJ*
691   4:e2539. 10.7717/peerj.2539
692   Clement AM, Mensforth CL, Challands TJ, Collin SP, and Long JA. 2021. Brain Reconstruction Across
693   the Fish-Tetrapod Transition; Insights from Modern Amphibians. *Frontiers in Ecology and*
694   *Evolution* 9:60. doi: 10.3389/fevo.2021.640345
695   Clement AM, Nysjö J, Strand R, and Ahlberg PE. 2015. Brain – endocast relationship in the Australian
696   lungfish, *Neoceratodus forsteri*, elucidated from tomographic data (Sarcopterygii: Dipnoi).
697   *PloS One* 10:e0141277. DOI: 10.1371/journal.pone.0141277

698 Clément G, and Ahlberg PE. 2010. The endocranial anatomy of the early sarcopterygian *Powichthys*
699   from Spitsbergen, based on CT scanning. In: Elliott DK, Maisey JG, Yu X, and Miao D, eds.
700   *Morphology, Phylogeny and Paleobiogeography of Fossil Fishes: honoring Meemann Chang*.
701   Munich: Dr. Friedrich Pfeil, 363-377.
702 Cloutier R, Clement AM, Lee MSY, Noël R, Béchard I, Roy V, and Long JA. 2020. *Elpistostege* and the
703   origin of the vertebrate hand. *Nature* 579:549-554. https://doi.org/10.1038/s41586-020-
704   2100-8
705 Cloutier R, and Schultze H-P. 1996. Porolepiform fishes (Sarcopterygii). 248-270.
706 Coates MI, and Friedman M. 2010. *Litoptychus bryanti* and characteristics of stem tetrapod
707   neurocrania. In: Elliott DK, Maisey JG, Yu X-B, and Miao D, eds. *Morphology, phylogeny and
708   paleobiogeography of fossil fishes*. München: Verlag Dr. Friedrich Pfeil, 389–416.
709 Cope ED. 1882. On some new and little known Paleozoic vertebrates. *Proceedings of the American
710   Philosophical Society* 30:221-229.
711 Dempster WT. 1935. The brain case and endocranial cast of *Eryops megacephalus* (Cope). *Journal of
712   Comparative Neurology* 62.
713 Downs JP, and Daeschler EB. 2020. A New Species of *Megalichthys* (Sarcopterygii, Megalichthyidae)
714   from the Upper Devonian (Famennian) of Pennsylvania, U.S.A., and a Report on the
715   Cosmine-Covered Osteolepiform Fossils of the Catskill Formation. *Journal of Vertebrate
716   Paleontology*. DOI: 10.1080/02724634.2020.1774771
717 Downs JP, Daeschler EB, Jenkins FAJ, and Shubin NH. 2008. The cranial endoskeleton of *Tiktaalik
718   roseae*. *Nature* 455:925-929.
719 Fox RC, Campbell KSW, Barwick RE, and Long JA. 1995. A new osteolepiform fish from the Lower
720   Carboniferous Raymond Formation, Drummond Basin, Queensland. *Memoirs of the
721   Queensland Museum* 38:97-221.
722 Giles S, and Friedman M. 2014. Virtual Reconstruction of Endocast Anatomy in Early Ray-Finned
723   Fishes (Osteichthyes, Actinopterygii). *Journal of Paleontology* 88:636-651.
724 Hay OP. 1902. Bibliography and catalogue of the fossil Vertebrata of North America (No. 179). *US
725   Government Printing Office*.
726 Henderson SAC, and Challands TJ. 2018. The cranial endocast of the Upper Devonian dipnoan
727   `Chirodipterus' australis. *PeerJ* 6:e5148. DOI 10.7717/peerj.5148
728 Holland T. 2014. The endocranial anatomy of *Gogonasus andrewsae* Long, 1985 revealed through
729   micro CT-scanning. *Earth and Environmental Science Transactions of the Royal Society of
730   Edinburgh* 105:9-34.
731 Janvier P, Clément G, and Cloutier R. 2007. A primitive megalichthyid fish (Sarcopterygii,
732   Tetrapodomorpha) from the Upper Devonian of Turkey and its biogeographical implications.
733   *Geodiversitas* 29:249-268.
734 Jarvik E. 1954. On the visceral skeleton in *Eusthenopteron* with a discussion of the parasphenoid and
735   palatoquadrate in fishes. *Almqvist & Wiksells* 5.
736 Jarvik E. 1972. Middle and Upper Devonian Porolepiformes from East Greenland with Special
737   Reference to *Glyptolepis groenlandica* n. sp. and a Discussion on the Structure of the Head in
738   the Porolepiformes. *Meddelelser om Gronland* 187:1-307.
739 Jarvik E. 1980. *Basic Structure and Evolution of Vertebrates*. London: Academic Press.
740 Johanson Z. 2004. Late Devonian sarcopterygian fishes from eastern Gondwana (Australia and
741   Antarctica) and their importance in phylogeny and biogeography. In: Arratia G, Wilson MVH,
742   and Cloutier R, eds. *Recent Advances in the Origin and Early Radiation of Vertebrates*.
743   Munich, Germany: Verlag Dr. Friedrich Pfeil, 287-308.
744 Johanson Z, and Ahlberg PE. 1997. A new tristichopterid (Osteolepiformes: Sarcopterygii) from the
745   Mandagery Sandstone (Late Devonian, Famennian) near Canowindra, NSW, Australia.
746   *Transactions of the Royal Society of Edinburgh: Earth Sciences* 88:39-68.

747   Johanson Z, and Ahlberg PE. 2001. Devonian rhizodontids and tristichopterids (Sarcopterygii;
748   Tetrapodomorpha) from East Gondwana. *Transactions of the Royal Society of Edinburgh:*
749   *Earth Sciences* 92:43-74.
750   Kardong KV. 2006. *Vertebrates: Comparative Anatomy, Function, Evolution*. New York: McGraw Hill.
751   King B, Hu Y, and Long JA. 2018. Electroreception in early vertebrates: survey, evidence and new
752   information. *Palaeontology*:1-34. doi: 10.1111/pala.12346
753   Lebedev OA. 1995. Morphology of a new osteolepidid fish from Russia. *Bulletin du Muséum national*
754   *d'Histoire naturelle, Paris 4e Série Section C Sciences de la Terre Paléontologie, Géologie,*
755   *Minéralogie* 17:287-341.
756   Long J, Clement AM, and Choo B. 2018. New insights into the origins and radiation of the mid-
757   Palaeozoic Gondwanan stem tetrapods. *Earth and Environmental Science Transactions of the*
758   *Royal Society of Edinburgh*:1-17. https://doi.org/10.1017/S1755691018000750
759   Long JA. 1985. A new osteolepid fish from the Upper Devonian Gogo Formation of Western
760   Australia. *Records of the Western Australian Museum* 12:361-377.
761   Long JA, Barwick RE, and Campbell KSW. 1997. Osteology and functional morphology of the
762   osteolepiform fish *Gogonasus andrewsae* Long, 1985, from the Upper Devonian Gogo
763   Formation, Western Australia. *Records of the Western Australian Museum Supplement* 53:1-
764   89.
765   Lu J, Zhu M, Ahlberg PE, Qiao T, Zhu Y, Zhao W, and Jia LT. 2016. A Devonian predatory fish provides
766   insights into the early evolution of modern sarcopterygians. *Science Advances* 2:1-8.
767   Lu J, Zhu M, Long JA, Zhao W, Senden TJ, Jia LT, and Qiao T. 2012. The earliest known stem-tetrapod
768   from the Lower Devonian of China. *Nature Communications* 3:1160. DOI:
769   10.1038/ncomms2170
770   Miles RS. 1977. Dipnoan (lungfish) skulls and the relationships of the group: a study based on new
771   species from the Devonian of Australia. *Zoological Journal of the Linnean Society* 61:1-328.
772   Nakane Y, Ikegami K, Iigo M, Ono H, Takeda K, Takahashi D, Uesaka M, Kimijima M, Hashimoto R,
773   Arai N, and Suga T. 2013. The saccus vasculosus of fish is a sensor of seasonal changes in day
774   length. *Nature Communications* 4:p.2108.
775   Pardo JD, Szostakiwskyj M, Ahlberg PE, and Anderson JS. 2017. Hidden morphological diversity
776   among early tetrapods. *Nature* 546:642-645. doi:10.1038/nature22966
777   Perilli E, Parkinson IH, and Reynolds KJ. 2012. Micro-CT examination of human bone: from biopsies
778   towards the entire organ. *Annali dell'Istituto superiore di sanita* 48:75-82.
779   Romer AS. 1937. The braincase of the Carboniferous Crossopterygian *Megalichthys nitidus*. *Bulletin*
780   *of the Museum of Comparative Zoology* 132:1-73.
781   Romer AS, and Parsons TS. 1985. *The Vertebrate Body*.
782   Säve-Söderbergh G. 1952. On the skull of *Chirodipterus wildungensis* Gross, an Upper Devonian
783   dipnoan from Wildungen. *Kunglinga Svenska Vetenskapsakademiens Handlingar 4* 3:1-29.
784   Schultze H-P. 2009. The international influence of the Stockholm School. *Acta Zoologica* 90:22-37.
785   Schultze HP. 1974. Osteolepidide Rhipidistia (Pisces) aus dem Pennsylvanian von Illinois/USA. *Neues*
786   *Jahrbuch für Geologie und Paläontologie, Abhandlungen* 146:29-50.
787   Simões TR, and Pierce SE. 2021. Sustained high rates of morphological evolution during the rise of
788   tetrapods. *Nature Ecology and Evolution*:1-12. https://doi.org/10.1038/s41559-021-01532-x
789   Snitting D. 2008. A redescription of the anatomy of the Late Devonian *Spodichthys buetleri* Jarvik,
790   1985 (Sarcopterygii, Tetrapodomorpha) from East Greenland. *Journal of Vertebrate*
791   *Paleontology* 28:637-655.
792   Stensiö E. 1963. The Brain and the Cranial Nerves in Fossil, Lower Craniate Vertebrates. *Skrifter utgitt*
793   *av Det Norske Videnskaps-Akademi*:1-120.
794   Thomson KS. 1964. Revised Generic Diagnoses Of The Fossil Fishes *Megalichthys* And
795   *Ectosteorhachis* (Family Osteolepidae). *Bulletin of the Museum of Comparative Zoology*
796   131:283-311.

797   Thomson KS, and Rackoff JS. 1974. The shoulder girdle of the Permian rhipidistian fish
798   *Ectosteorhachis nitidus* Cope: structure and possible function. *Journal of Paleontology*
799   48:170-179.
800   Thomson KS, and Vaughn PP. 1968. Vertebral structure in Rhipidistia (Osteichthyes, Crossopterygii)
801   with description of a new Permian genus. *Peabody Museum of Natural History* 127:1-19.
802   Vorobyeva EI. 1975. An osteolepid crossopterygian from the Ketleri Formation of Latvia. In: A. GA,
803   ed. *Fauna and Stratigraphy of the Palaeozoic and Mesozoic of Baltics and Byelorussia*.
804   Mintis, Vilnius, 233–237.
805   Vorobyeva EI. 1977. Morphology and evolution of sarcopterygian fishes. *Trudy*
806   *Paleontologischeskogo Instituta Akademia, Nauk SSSR* 163:1-239.
807   Witzmann F, and Schoch RR. 2012. A megalichthyid sarcopterygian fish from the Lower Permian
808   (Autunian) of the Saar-Nahe Basin, Germany. *Geobios* 45:241-248.
809   Young GC, Long JA, and Ritchie A. 1992. Crossopterygian fishes from the Devonian of Antarctica:
810   systematics, relationships and biogeographic significance. *Records of the Australian Museum*
811   Supplement 14:1-77.
812   Zhu M, and Ahlberg PE. 2004. The origin of the internal nostril of tetrapods. *Nature* 432:94-97.
813   10.1038/nature02843
814   Zhu M, Ahlberg PE, Zhao W-J, and Jia L-T. 2017. A Devonian tetrapod-like fish reveals substantial
815   parallelism in stem tetrapod evolution. *Nature Ecology and Evolution*. DOI: 10.1038/s41559-
816   017-0293-5

817

Figure 1

Figure 1. Micro-CT 3D rendering (58 µm pixel size) of dermal skull and braincase of *Cladarosymblema* (QMF 21082).

A, skull in dorsal view showing placement of bones on holotype; B, braincase in ventral view; dermal skull bones, braincase and palatal bones in C, dorsal and D, ventral view; E, skull and cheek in right lateral view.

A

Sensory line canal
Intracranial joint
Parietal shield
Postparietal shield
Cheek bones
Sub-opercular
20 mm
Median extrascapular
Operculum

B

Premaxillary tusk
Apical fossa
Nasal capsule
Parasphenoid
Bucco-hypophysial foramen
Skull roof
Basicranial fenestra
Otic shelf
Hyomandibular articulation
Otic capsule
Notochordal canal
10 mm

C

Sub-opercular
Operculum
Supratemporal anterolateral process

D

Vomer
Premaxilla
Dermopalatine
Vomer articulation area
Ectopterygoid
Palatoquadrate
Oticoccipital
Subopercular
20 mm

E

Preopercular?
Squamosal?
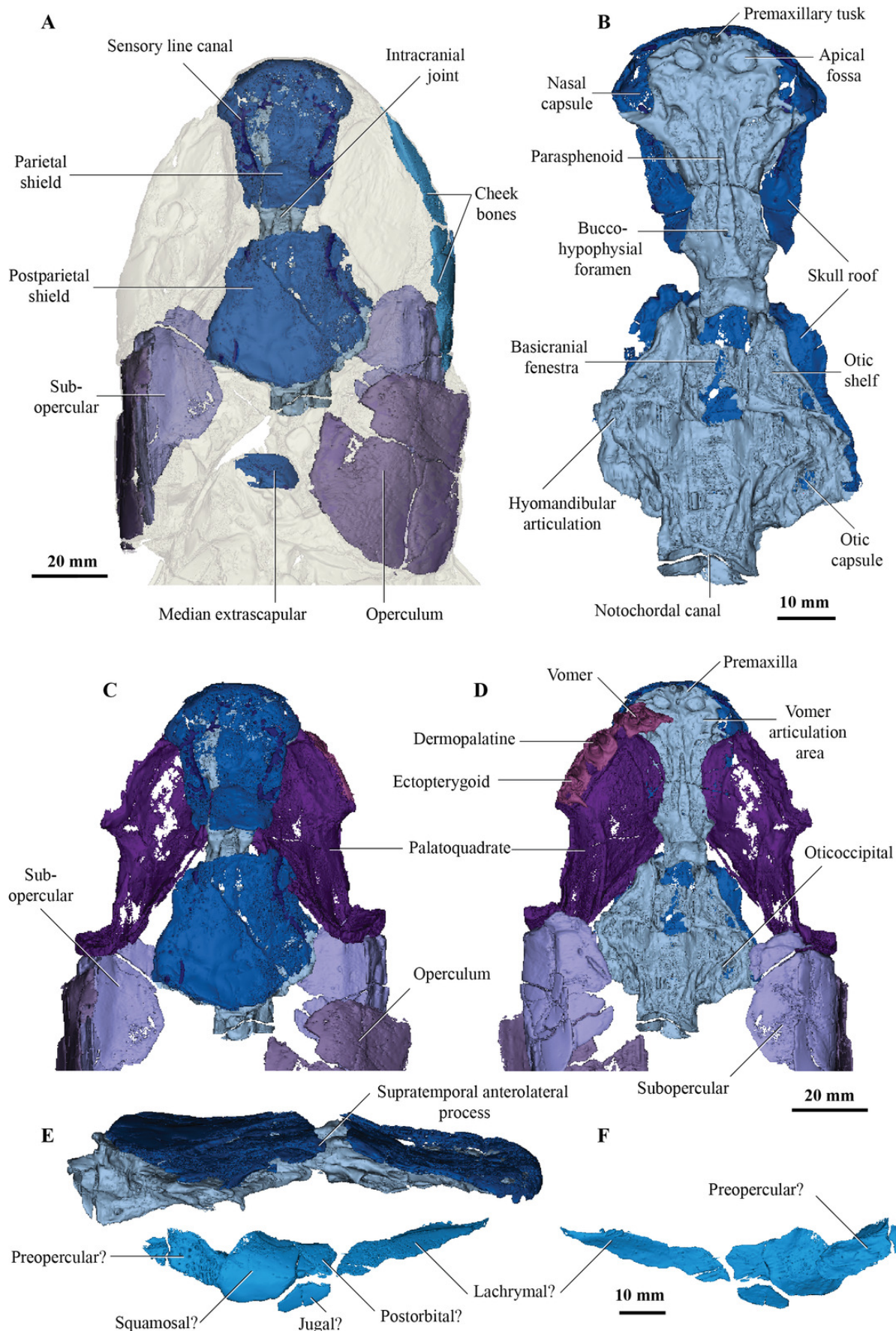Jugal?
Postorbital?
Lachrymal?

F

Preopercular?
10 mm

Figure 2

Figure 2. Micro-CT 3D rendering (58 μm pixel size) of mandible and submandibular bones of *Cladarosymblema* (QMF 21082).

A, mandibular bones in ventral view showing placement of bones on holotype; mandible in B, dorsal; C, lingual; and D, labial view.
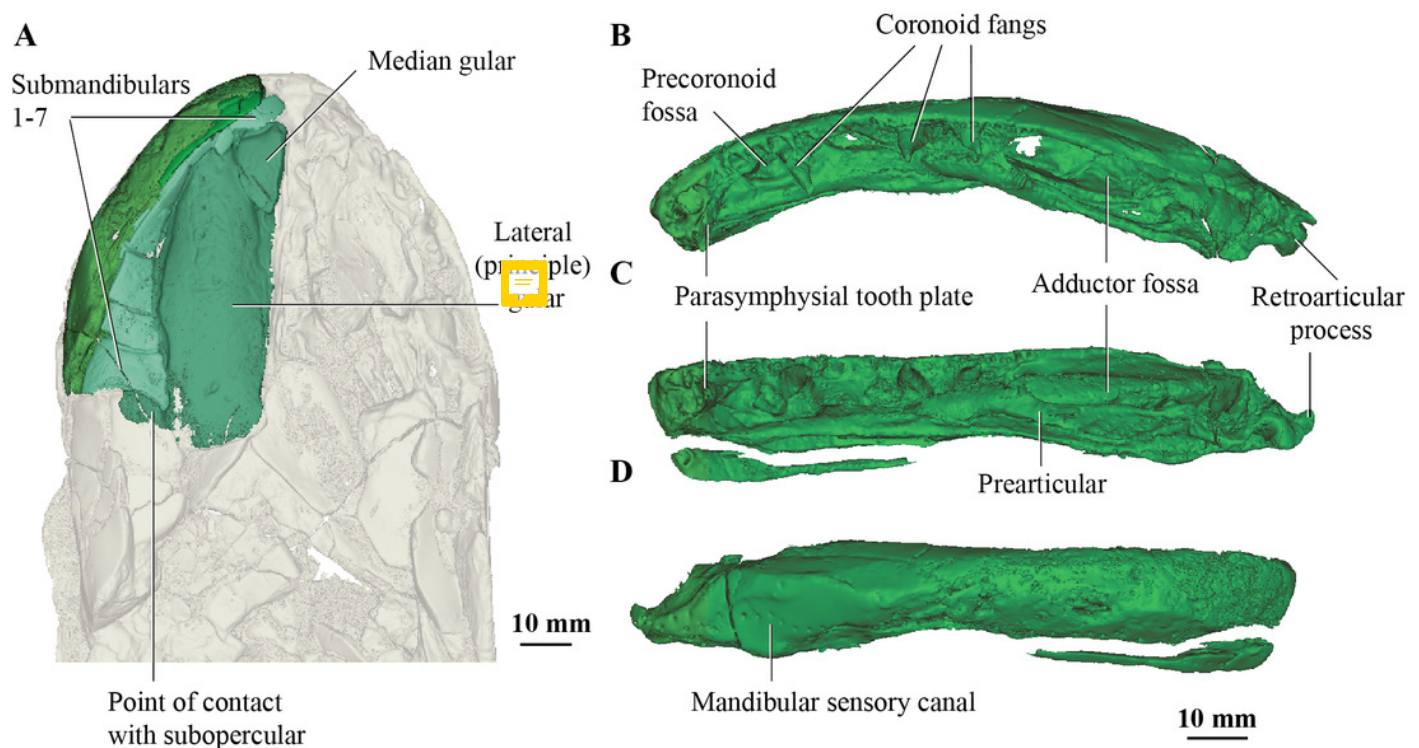
Figure 3

Figure 3. Micro-CT 3D (58 μm pixel size) and synchrotron rendering (12 μm pixel size) of cranial endocast and sensory lines of *Cladarosymblema* (QMF 21082).

A, dorsal; b, ventral; and C, left lateral view; QMF 21083 in D,E, dorsal view; F,G, ventral view; H, left lateral view showing zoomed in hypophysial fossa region.

A — Infraorbital sensory line canal; Supraorbital sensory line canal; Optic nerve canal (n.II); Postition of posterior semicircular canal; Vagus nerve canal (n.X); Supraotic cavities; Supratemporal commissural sensory line canal

B — Sacculus; Notochordal canal; 10 mm

C — Olfactory canal (n.I); Pineal eminence; Supraotic cavities; Hypophyseal fossa; Notochordal canal; 10 mm

D

E — Nasal capsule; Sensory line canal; Optic nerve canal (n.II); Olfactory tract canal (n.I); Skull roof

F — 10 mm

G — Nasal capsule; Orbitonasal vein; Olfactory tract canal (n.I); Optic nerve canal (n.II); Bucco-hypophyseal foramen; Hypophyseal fossa

H — Optic nerve canal (n.II); 10 mm; Hypophyseal fossa; Nasal capsule; Optic nerve canal (n.II); Opthalmic artery canals; Hypophyseal fossa; Internal carotid artery; Palatine artery canals; Buccohypophyseal foramen; 5 mm
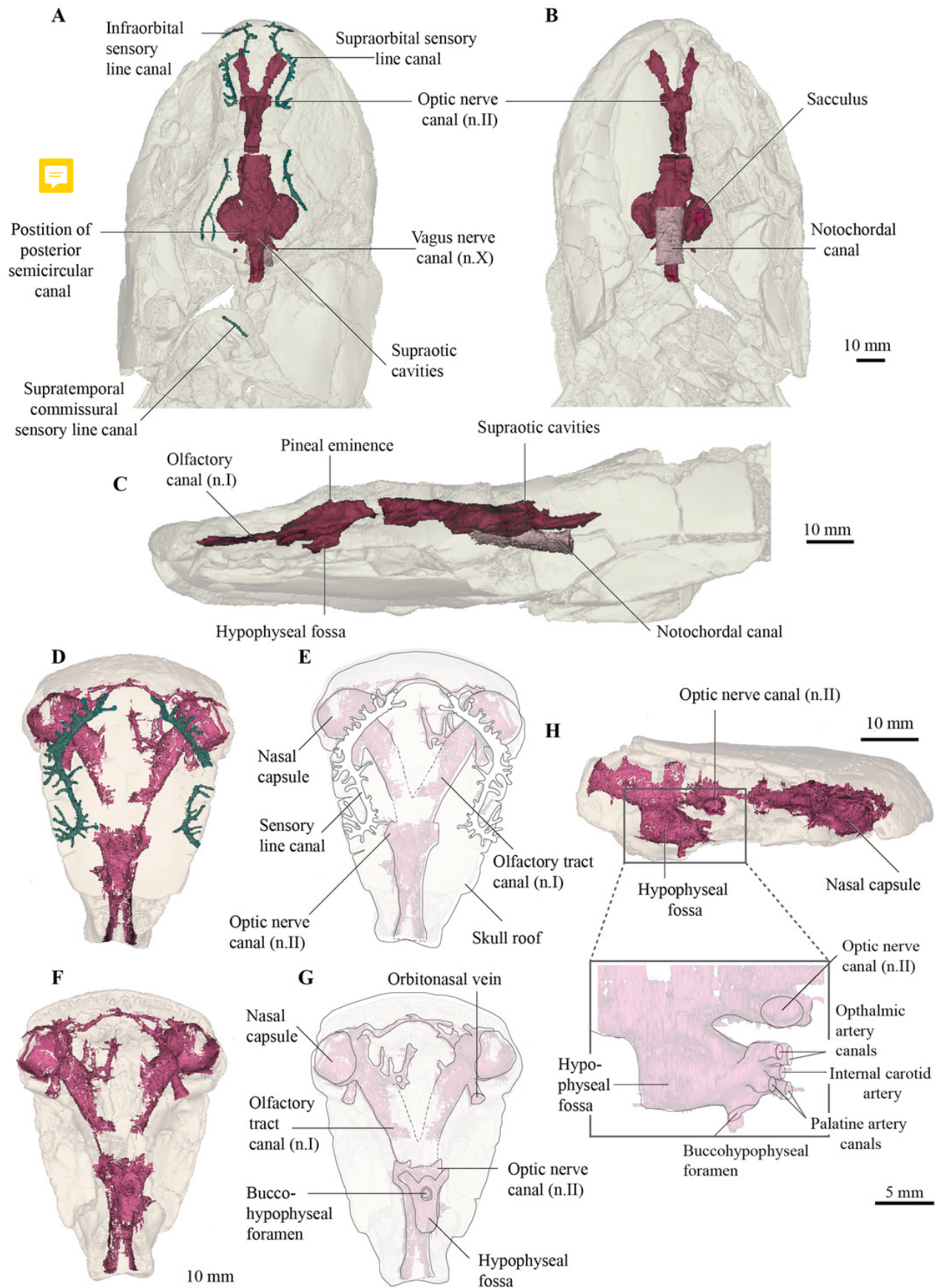
Figure 4

Figure 4. Micro-CT 3D rendering (58 μm pixel size) of hyoid and branchial skeleton of *Cladarosymblema* (QMF 21082).

A, skull in dorsal view showing placement of bones on holotype; B, in ventral view; C,D, full hyoid and basibranchial skeleton including ceratobranchials as preserved *in situ*.

A

B

20 mm

C

Hypohyal

Hypo-
branchials 1-3

Basibranchial

Hyo-
mandibular

4th
Hypobranchial

D

Hypohyal

Sublingual rod

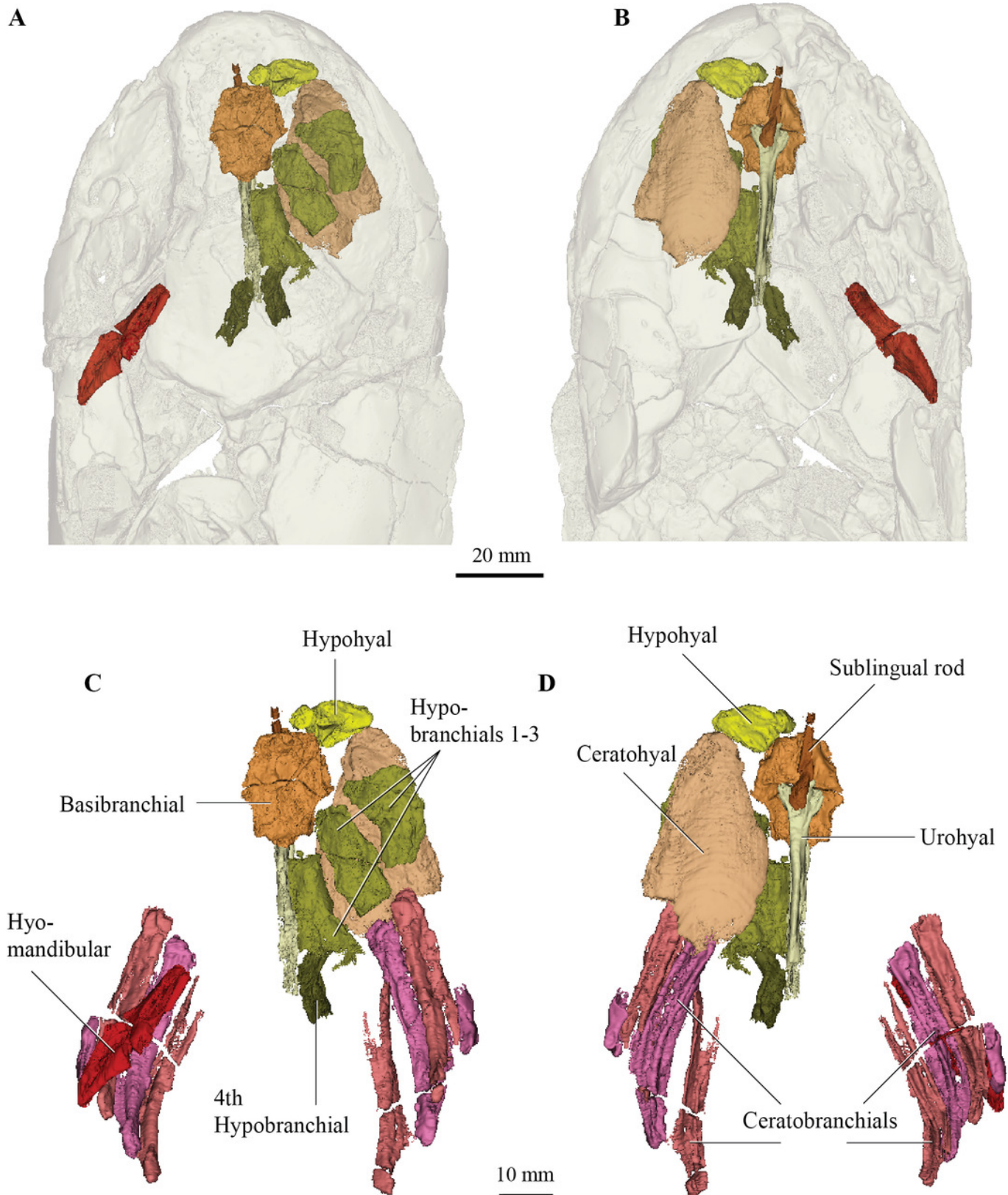Ceratohyal

Urohyal

Ceratobranchials

10 mm

Figure 5

Figure 5. Micro-CT 3D rendering (58 μm pixel size) of pectoral and axial elements of *Cladarosymblema* (QMF 21082).

A, ventral view, and B, in dorsal view, showing placement of bones on holotype; pectoral girdle in C, dorsal view; and D, ventral view; E, F, anocleithra in alternate views; and neural arches in G, lateral; I, dorsal; K, ventral view; ring centra in H, lateral; J, dorsal; L, ventral view.

A

B

30 mm

C

Inter-
clavicle

Branchial
lamina

Anocleithrum

Cleithrum

20 mm

D

Clavicle

Scapulocoracoid

Anocleithrum

E

Anocleithrum

F

Anocleithrum

10 mm

G

Neural spine

H

I

J
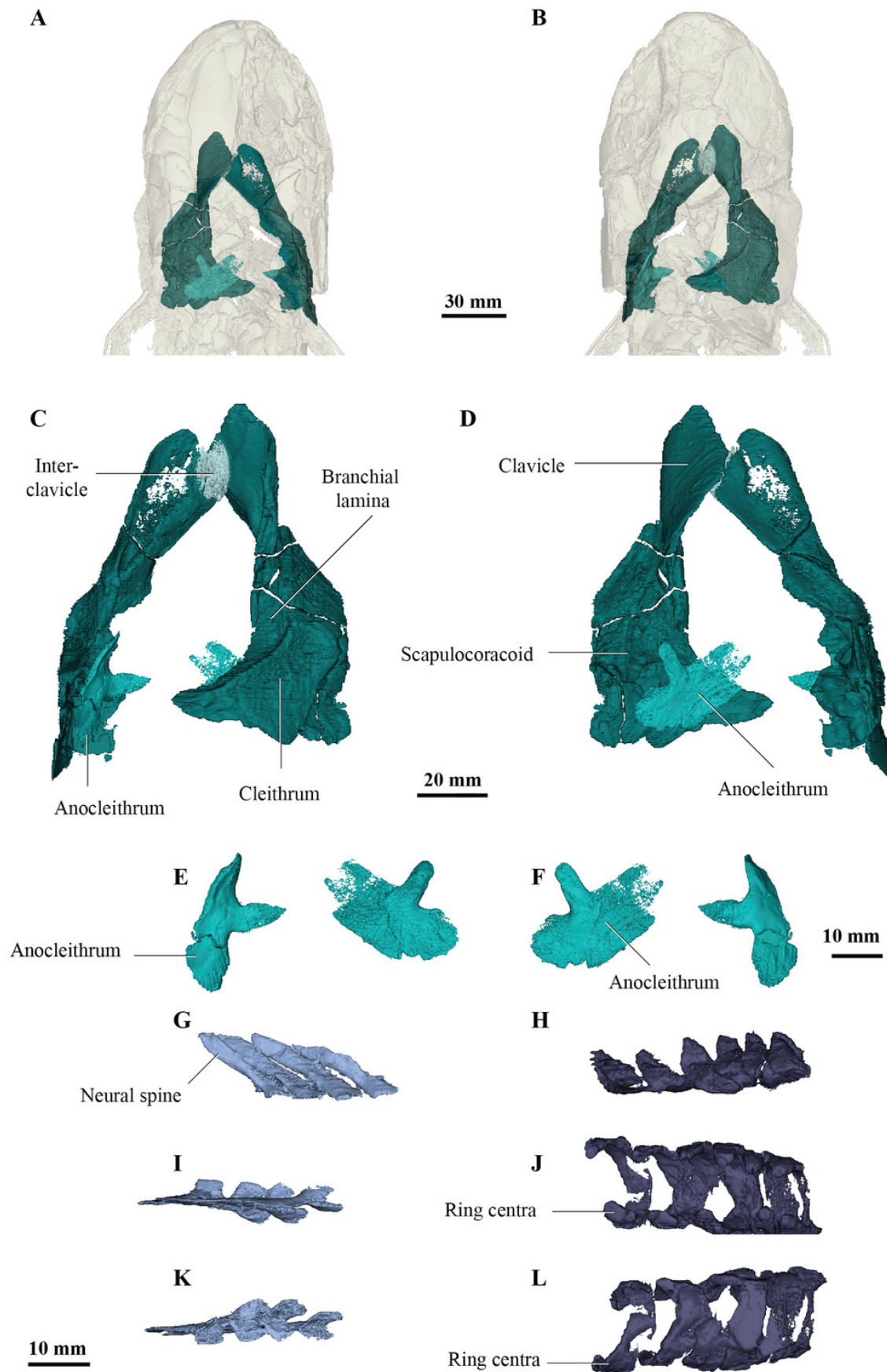
Ring centra

K

10 mm

L

Ring centra

Figure 6

Figure 6. Parsimony analyses.

A, 50% majority-rule consensus tree from parsimony analysis with inclusion of all taxa showing monophyly of the Megalichthyidae; B, Canowindrid + Megalichthyid sub-set with most incomplete taxa excluded (*Mahalalepis, M. mullisoni, M. laticeps, Sengoerichthys*) provides greater resolution of megalichthyid phylogeny. Image silhouettes are authors own (elpistostegalids, rhizodonts, megalichthyid) or from PhyloPic http://phylopic.org/ (*Ichthyostega*, Scott Hartman; *Eusthenopteron* & *Gogonasus*, Michael Keesey).
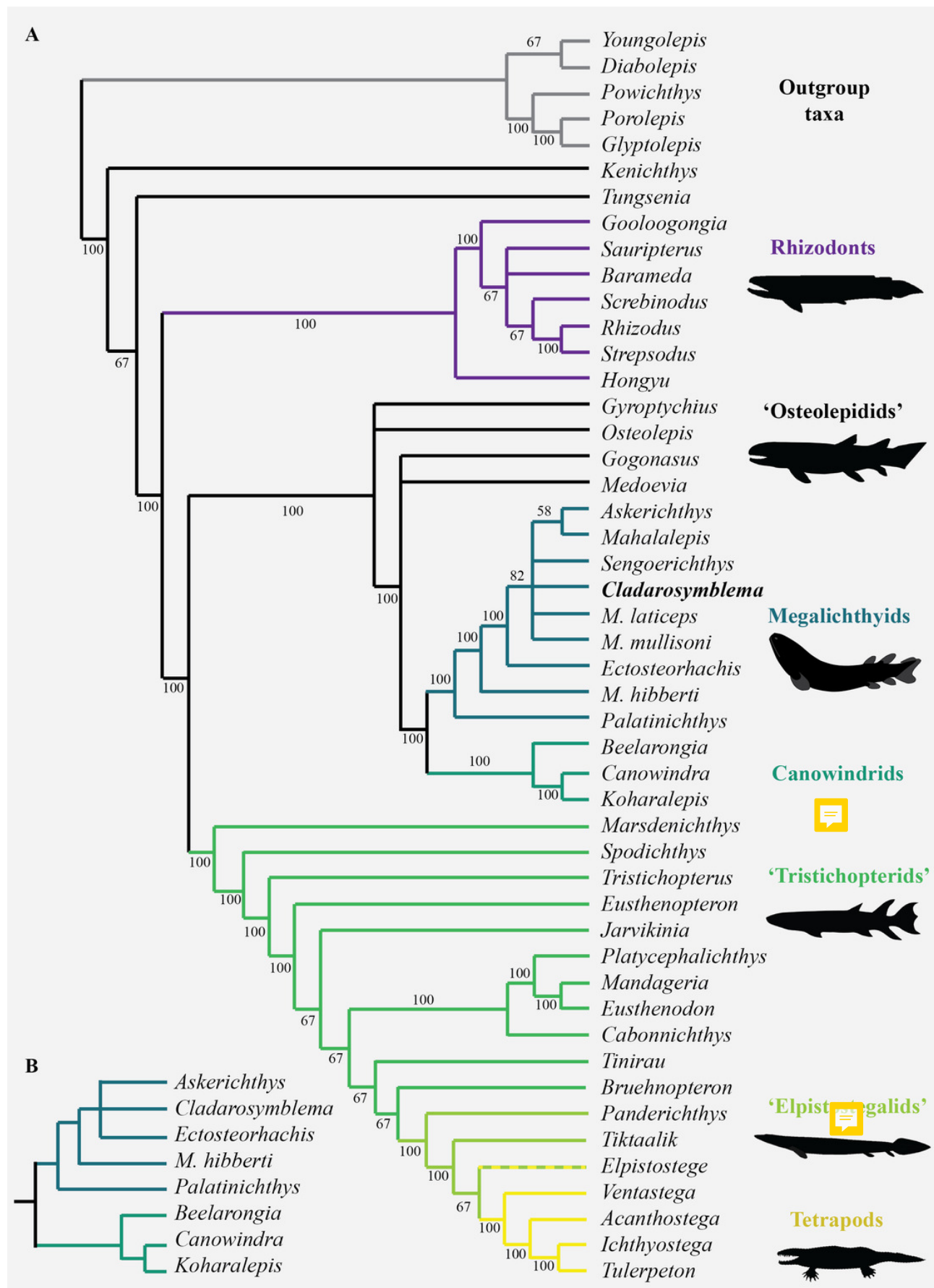
Figure 7

Figure 7. Lateral head reconstruction of *Cladarosymblema.*

Compiled from Fox et al. (1995) and new data presented herein. Colour-coded as follows: dermal skull roof (dark blue), cheek (light blue), lower jaw (pale green), opercular series (purple), and pectoral (dark green). Bones marked with "?" remain unknown in this taxon.